Surface evidence of active tectonics along the Pergola-Melandro fault: a critical issue for the seismogenic potential of the southern Apennines, Italy.

Marco Moro[1]*, Laura Amicucci[1], Francesca R. Cinti[1], Fawzi Doumaz[1], Paola Montone[1], Simona Pierdominici[1], Michele Saroli[1], Salvatore Stramondo[1] and Boris Di Fiore[2]

[1] *Istituto Nazionale di Geofisica e Vulcanologia, via di Vigna Murata 605 – 00143 Rome, Italy.*

[2] *Dipartimento di Scienze - Università di Napoli, "Federico II", via Cintia - 80126 Naples, Italy.*

---

* *Corresponding author.*

E-mail addresses: moro@ingv.it

Abstract

The Pergola-Melandro basin (southern Apennines) is characterized by a below-average release of seismic energy within a wider earthquake-prone region. In fact, it is placed between the maximum intensity areas of two of the most destructive earthquakes reported in the Italian seismic catalogue: the M ≥ 7.0 Agri Valley earthquake in 1857 and the Ma = 6.9 Irpinia earthquake in 1980. In this work, we present geomorphologic analysis, electrical resistivity surveys and field data, including paleoseismologic evidence, that provided the first direct constraints on the presence of a ~20 km long, seismogenic fault at the western border of the Pergola-Melandro basin. We also obtained geological information on the recent deformation history of the Pergola-Melandro fault that indicates the occurrence of at least four surface faulting earthquakes since Late Pleistocene age. The empirical relationships linking fault length and magnitude would assign to the Pergola-Melandro fault an event of M ≥ 6.5. These new data have important implication on the seismic hazard assessment of this sector of the Apennines, that also includes large cities such as Potenza, about 20 km far from the recognized Pergola-Melandro fault, and highlight the relevance of the geological approach in areas where the seismological records are poor. Finally, we discuss the

Pergola-Melandro fault within the regional seismotectonic context. In particular, this fault belongs to the system of normal faults with an apenninic orientation, both NE and SW dipping, that accommodate the NE- crustal extension taking place in the area. Nearby faults, similarly oriented but with opposite dip, may coexist whether linked by secondary faults that act as slip transfer structures. This complex system of active faults would be more realistic than to consider a narrow band of faults, running along the belt axis, with an homogenous geometry and, moreover, more consistent with the high extension rate measured by historical earthquakes and geodetic data.

Keywords: Lucanian Apennine; seismogenic fault; surface faulting; seismic hazard

1. Introduction

The Lucanian Apennine represents one of the most seismically active portion of the belt being repeatedly hit by large-moderate earthquakes in historical and instrumental time. In order to contribute to the understanding of the seismogenic potential within the Lucanian Apennine (Fig. 1), we focused our study in the Pergola–Melandro basin, a poorly-known area from an active tectonics point of view. In fact, the Pergola-Melandro (hereinafter referred to as PM) basin is located in between the epicentral zones of two large seismic events: the 1980 Irpinia earthquake to the north and the 1857 Agri Valley seismic event to the south (Fig. 1 and Table 1). The Irpinia fault, responsible for the 1980 seismic event, has been widely studied (i.e. Pantosti et al., 1993) and identified as a NW-SE trending normal fault, NE-dipping; the 1857 mainly normal fault has been located by most of the authors within the Agri Valley although the geometry (dipping, strike and location) of the main fault is still strongly debated (Benedetti et al., 1998; Cello et al., 2003; Maschio et al., 2005). Within the PM basin, the literature does not report any clear and detailed mapping of a surface seismogenic fault trace nor the historical events of the area (1561 and 1826 seismic events) are definitively attributed to local faults (Fig. 1). The 1561 is the largest earthquake

(Ma = 6.4) occurring just west of the PM basin; at present the responsible fault is hypothetically attributed to the NW-SE Caggiano fault (Fig. 1; Galli et al., 2006).

After a brief description of the geological and seismotectonic setting of the area, we present new surface and shallow subsurface data (stratigraphic, geomorphological and geophysical) that allowed us to identify a seismogenic fault, bounding the western edge of the basin. The recent activity of the fault is also constrained by new radiocarbon dating. The final part of the paper is dedicated to a discussion on the fault parameters evaluated on the basis of the collected data and on the system of active faults delineated within the Lucanian sector of the Apenninic belt.

2. Geological and seismotectonic framework

The geodynamic setting of the Italian region is the result of the NNW-SSE convergence between Africa and Eurasian plates (De Mets et al., 1990), although the peninsular sector is presently undergoing NE-SW extension perpendicular to the Apenninic fold and thrust belt (Anderson and Jackson, 1987; Westaway, 1992; Pondrelli et al., 1995; Amato and Montone, 1997). In particular, the southern Apennines are a NE-verging fold-and-thrust belt (Mostardini and Merlini, 1986; see also Fig. 5 in Meletti et al., 2000), built on the western border of the Apulian plate from Late Oligocene-Early Miocene times (Pescatore et al., 1999). The belt is composed of a Mesozoic-Cenozoic sedimentary succession from different palaeogeographic domains and of the Neogene-Pleistocene piggyback basins and foredeep deposits of the active margin.

The PM basin is a Quaternary tectonic depression within the Lucanian Apennine (southern Italy) (Figs. 1 and 2). Starting from Late Oligocene-Early Miocene times, this portion of the Apennines was characterized by the eastward propagation of thrusts, that piled up the Apenninic carbonate platform on the Lagonegro pelagic basin successions (Mostardini and Merlini, 1986; Monaco et al., 1998; Casero et al., 1992; Menardi Noguera and Rea, 2000; Merlini and Cippitelli, 2001). During Late Pliocene-Early Pleistocene, the axial zone of the belt was affected by mainly strike-slip fault systems with N120, N50-60, and N-S oriented structures (Cinque et al., 1993;

Schiattarella et al., 2003; Giano and Martino, 2003). Recent shortening occurred at the belt front and ceased in Middle Pleistocene (e.g. Pieri et al., 1997; Patacca and Scandone, 2004). The latest and still active tectonic episode within the belt is represented by a NE-SW extensional regime governed by high angle normal faults that match the Apenninic orientation, and evidenced by geophysical (Amato and Montone, 1997; Pondrelli et al., 2002; Frepoli and Amato, 2000), geological (Benedetti et al., 1998; Cinque et al., 2000; Galadini et al., 2000; Montone et al., 2004; DISS Working Group, 2005; Maschio et al., 2005; Galli et al., 2006) and geodetic data (D'Agostino et al., 2001; Hunstad et al., 2003).

Different interpretations have been proposed for the genesis of the PM basin. Some authors consider the PM basin as related to strike-slip tectonics (Schiattarella et al., 2003; Giano and Martino 2003). Giano and Martino (2003) highlight the presence of two fault systems: one with a strike slip kinematics (N60-80) that likely is sin-sedimentary during the Early Pleistocene, the other with a normal kinematics (N160-170) that cuts the whole stratigraphic succession. However, Santangelo (1991) suggests that the actual landscape is the result of two normal faulting stages. The PM basin can be stratigraphically divided in 2 sub-basins: the S. Angelo sector to the north and the Brienza to the south, separated by an anti-Apenninic structural high near Brienza village (Fig. 2, Lippmann-Provansal, 1987; Santangelo, 1991), while Giano and Martino (2003) show the continuity of the two sub-basins after the Middle Pleistocene. In this context, the PM basin was filled with fluvio-lacustrine deposits reaching a thickness of 80-150 m (Santangelo, 1991; Giano and Martino, 2003).

From a seismotectonic point of view, the Lucanian Apennine represents an active region where the historical seismic catalogue (CPTI Working Group, 2004) reports three large historical earthquakes within and very close to the PM basin: the 1561, 1826 and 1857 earthquakes. Further large events occurred outside the study area, i.e. the 1694, the 1836 south of the Agri Valley, and the 1980 event north of the PM basin (Fig.1 and Table 1). During the last 25 years the PM basin was characterized by a poor and diffuse low-magnitude seismicity (Fig. 1; Castello et al., 2005,

Frepoli et al., 2005), in contrast with the neighbourhood areas that experienced four seismic sequences (Table 1): the Potenza 1990 and 1991 (Ekström, 1994), the Irpinia 1996 (Cocco et al., 1999), the Savoia di Lucania 2002 (Cucci et al., 2004; Frepoli et al., 2005). In particular, the Savoia di Lucania sequence occurred just north of the PM basin and the CMT solution of the mainshock indicates a prevailing normal faulting mechanism with ~NE–SW direction of extension, confirmed also by the breakout analysis (Cucci et al., 2004; Montone et al., 2004). The seismotectonic pattern delineated within the PM basin is then characterized by extensional regime with T-axes and Sh_{min} mainly NE-SW oriented. These data are also in agreement with geodetic studies showing a continuity of strain accumulation with a NE-SW extensional principal strain axis in the Lucanian Apennine (Hunstad et al., 2003).

3. The Pergola-Melandro fault: surface and shallow subsurface data

3.1 Geomorphology, field geology and absolute datings

Aerial images, DEM and field observations were used to reconstruct the surface expression of the PM fault and to define its recent activity. From our analysis we have recognized the PM fault as a ~ 20 km long, mainly normal fault, ENE downthrown side, running on the western edge of the PM basin (Fig. 2).

For most of its length, the fault trace (Fig. 2) corresponds to a change in the slope dip and it is also locally expressed as scarplets at the footslope, as high as 3 m, in alluvial and colluvial deposits (Fig. 3a, b). The PM fault is composed of two main segments arranged in a left en-échelon pattern (Fig. 2).

From north to south, the first fault segment is ~8 km long, has an average strike of N320 that gently rotates to N340. It is expressed by NNW-SSE limestone fault plane with main dip-slip striae, which is in tectonic contact with Quaternary colluvial slope deposits. At several sites, slope deposits of about 15 kyr appear strongly sheared and tilted (Fig. 3c), testifying the recent activity of this portion of fault. The southernmost 3 km of this segment overlaps the southern fault trace that steps

~3 km toward northeast. Here, the PM fault at surface has a trend of N320 that gradually reaches N350. The 13 km-long southern fault trace is better preserved and the evidence of recent activity are well recorded in the stratigraphy respect to the northern segment. This different surface expression of the fault is related to the deeper erosion affecting the northern portion of the basin caused by the presence of the morpho-structural threshold of the *Coste San Salvatore* range (Fig. 2). Natural outcrops and quarries expose loose sediments such as alluvium, colluvium and slope deposits of Pleistocene-Holocene age that are deformed and involved in the fault activity.

We describe in detail the fault zone exposed within a quarry just west of Pergola village (Fig. 2), where the trace branches into four main sub-parallel strands (F1, F2, F3, F4 in Figs. 4 and 5). The quarry intersects two of these (Fig. 5) and was carved in two postglacial alluvial fans placed on the hanging wall of the fault, as reconstructed from the aerial photo (Fig. 4). The stratigraphy of the wall and the structures within the deposits lead to the recognition of two zones of deformation at different elevation: upper fault F2 and lower fault F1. F2 is located at the topographic change of the slope and it is characterized by a ~75° east dipping, tectonic contact between cataclastic dolomia (Trias) and Upper Quaternary deposits (Fig. 6). The latter consist of colluvium and paleosoils with a subvertical attitude that are strongly sheared in the 2 m observable exposure. The sequence is truncated to the top by an erosional surface capped by undeformed organic silt deposits. The pedogenic brown colluvium within the zone of deformation and the undeformed organic silt have an age of 8204-7745 B.C. and 1772-1520 B.C., respectively (Table 2). Twenty meters far from this zone and topographically below, the ~8 m-high wall of the quarry exhibits the zone of deformation F1 (Fig. 7), where the most useful information are collected. The top of the wall is at least 3 m below the actual topographic surface because of the presence of a quarry service road. The zone of deformation F1 is represented by a graben-structure with a main 1.5 m-wide sheared zone, ~65° east dipping (Fig. 7), that reaches the top of the wall, and with antithetic structures displayed in 6 m, that terminate upwards at different levels. The total width of the graben is 10 m. The graben-filling units consist of distinct layers of mainly medium to fine grained colluvial deposits partially

pedogenized alternating with paleosoils, containing varying amounts of silt and sand from slope materials, tephra and cataclastic dolomia. These deposits are faulted and tilted across the main and antithetic faults. The stratigraphic and structural setting evidence that the graben is a growing structure resulting from repeated surface faulting events and that the subsided area migrated with time. Stratigraphic indicators and features of deformation, such as angular discordances, sediments pinching out against the fault, increasing displacement with depth and upward-terminating faults, highlighted the occurrence of at least 4 events of faulting. The main fault and the antithetic ones activated during the oldest recognizable event and displaced the stratigraphic sequence up to paleosoil (A unit) (Fig. 7). Based on the age of A unit the event occurred shortly after 11594-11211 B.C. (Table 2). The A unit is vertically offset of a minimum cumulative amount of ~3.5 m across the graben. The subsided area was filled until a subsequent event of deformation truncated the surface that, at that time, was the pedogenic brownish silty colluvium (B unit), dated 8476-8257 B.C. (Table 2). As before, the newly formed graben area was completely filled and then sedimentation went through the structure. Some branches belonging to the main fault zone terminate upward within C unit, a reddish sandy-silty colluvium rich in volcanic material. This evidence and the lowest degree of deformation of the deposits in between B and C units, with respect to the oldest deposits, suggest the occurrence of a third event. Assuming that C unit was the surface at the time of occurrence, the deformation event is younger than 5639-5480 B.C. (Table 2). The most recent recognizable event displaced and deformed the entire stratigraphic sequence identified in this part of the quarry. The sheared zone clearly reaches the top of the carved wall and the deposits younger than C unit are less deformed. We cannot identify the undeformed youngest unit within the stratigraphic sequence of the quarry wall. However, in order to infer the first episode of sedimentation not interested by tectonic deformation at this site (F1), we can use the age of the undeformed organic silt (Table 2) sampled from the upper fault F2 (1772-1520 B.C.). Based on the stratigraphic characteristics of the sediment and on its location, the dated undeformed unit reasonably belongs to the upper portion of the post-glacial alluvial fan that covers the hanging wall

of the fault zone F2, as interpretable from the aerial photo in Fig. 4. This setting is in agreement with that exposed in a 2 m deep trench dug within the alluvial fan surface, ~20 m far south from the quarry wall (Fig. 5), that showed undeformed deposits.

3.2 Electrical resistivity profiles

Electrical resistivity (ER) data were acquired across F1 and F2 to investigate on possible horizontal and vertical discontinuities due to different materials or soil conditions. The ER depends on the porosity and permeability of the subsurface system, on the pore water and on the temperature (Llera et al., 1990). The instrumentation used is the IRIS-Syscal R2 High depth Resistivity-meter. The acquisition profile is composed by 48 electrodes, 1.5 m spaced both in Dipole-Dipole and Wenner configuration. The apparent resistivity data have been inverted by means of the RES2DINV software (Loke and Barker, 1996), also including the topography with low values of RMS (6% Dipole-Dipole and 2% for Wenner). Here, we show and discuss the most representative 2-D inversion of electrical resistivity data (profile 1 in Fig. 5).

In both the acquired configurations of Figure 8, it is defined a sharp and steep dipping resistivity discontinuity at least down to 8 m, that is in correspondence with the surface trace of F2. Below the F1 trace, a second electrical discontinuity between meters 30-35 of the profile is identified, suggesting the presence of the fault at depth. Moreover, the location and the resistivity values of this discontinuity are in agreement with the master fault recognized within the quarry, about 50 m northwest (Figs. 5 and 7). At this section, the structure resulting from the ER has a geometry resembling that of the graben of the quarry wall (Figs. 7 and 8).

4. Discussion and Conclusion

4.1 *The fault parameters*

Geomorphologic and structural analysis, radiocarbon dating and electrical resistivity survey provided the first direct constraints on the presence of a seismogenic fault bounding the western

edge of the PM basin. We also obtained information on the recent deformation history of the newly recognized fault. At the surface, the PM fault is ~20 km long, composed by two main segments with a left-stepping geometry, N320-N350 trending (Fig. 2 and Table 3). The kinematics of the fault is mainly normal, ENE downthrown side, though some lateral component of movement is hypothesized on the base of the complex shear zone observed at different sites. The main geometric characteristics of the PM fault, at depth, are coherent with those constrained by Lucente et al. (2005), that from unusual features in teleseismic receiver function revealed the presence of a dipping interface in the shallow crust interpreted as a fault.

Mostly from the structural and stratigraphic analysis of the deformation zone exposed at a quarry, we are able to estimate some kinematics parameters of the PM fault, described in the following and summarized in Table 2. Several structural features indicate the occurrence of at least 4 events of faulting in the last 13000 years along the southern segment of the PM fault. A *minimum vertical long term slip-rate* of ~0.26 mm/yr is tentatively estimated based on the age of A unit (11594-11211 B.C.) and on its minimum vertical offset across the graben (3.5 m). Our value is in agreement with that deduced by Schiattarella et al. (2003) from the analysis of erosional landsurfaces in the Lucanian Apennine (0.3-0.5 mm/yr in the time span of 1.8-1.2 Ma). Moreover, using the age (0.73 Ma) and the vertical displacement (140 m) of landsurface S3 across the PM fault, Schiattarella et al. (2003) infer a comparable slip-rate of ~0.2 mm/yr.

Based on the available radiocarbon ages of the deposits representing the surface at the time of the earthquake occurrence, we can roughly assume a *recurrence time* of ~3 kyr for surface faulting events. This value is in agreement with the behavior of other seismogenic faults in central-southern Apennines derived from paleoseismological investigations (e.g. Pantosti et al., 1993; Cinti et al., 1997; Michetti et al., 1997; Benedetti et al., 1998; Galli and Bosi, 2002). The oldest undeformed deposit was detectable only at the upper fault zone F2 of the quarry site; if we use its age (1772-1520 B.C.) and assume that F1 and F2 move always together, a *minimum elapsed time* of ~3.5 kyr is obtained: this value would approximate the recurrence time and consequently the probability of

reactivation for this structure would be very high. However we cannot exclude that F1 and F2 do not move together, but the most recent activity might be occurred along F1. Using the vertical displacement cumulated by the unit A (3.5 m) following the events of faulting (at least 4 events), a *maximum slip per event* of 0.87 m is inferred. On the base of the empirical relationships from Wells and Coppersmith (1994), we associate to the PM fault an expected magnitude larger than 6.5.

The new definition of the parameters regarding the geometry and the time behavior of the Pergola-Melandro fault represents an additional input for a more accurate seismic hazard assessment of the Lucanian sector of the Apennines, that also includes large cities such as Potenza, about 20 km far from the Pergola-Melandro basin. In addition, the direct evaluation of parameters to assign at each single seismogenic fault is particularly helpful for probabilistic seismic hazard computations (i.e. Cinti et al., 2004; Pace et al., 2006).

4.2 *The Pergola-Melandro fault in the regional seismotectonic context*

From a regional point of view, beyond the different dip direction of the mapped master seismogenic faults, active stress data (i.e., Montone et al., 2004) show that the southern apenninic belt is mainly affected by extensional deformation. This extensional pattern seems to be continuous and geometrically coherent throughout the tectonic history of the Lucanian region, from Late Pliocene to Present (Barchi et al., 2006). Through the analyses of seismic profiles, Barchi et al. (2006) show that the main basins of the area, such as the Vallo di Diano, the Agri Valley, Tanagro Valley and also the PM basins (see Fig. 1 for locations), have a similar half graben geometry, driven by SW-dipping normal faults for the Vallo di Diano and Agri Valley and NE-dipping normal fault for the Tanagro. The presence of adjacent normal faults similarly oriented but with opposite dipping (NE or SW) recurs in the Lucanian region (see i.e. Irpinia and Caggiano faults, Tanagro Valley, PM basin, Vallo di Diano and Agri Valley, in Fig. 1). The normal fault segments that accommodate the crustal extension taking place in the area, are possibly linked by differently oriented zone of slip transfer. In fact, according to Barchi et al. (2006), for the master faults bounding the Tanagro Valley

(Auletta basin) and Vallo di Diano, the stratigraphy of the syntectonic sediments filling the valleys, indicates that the activity of these opposite dipping faults has been synchronous at least for the Early-Middle Pleistocene time interval. The synchronous activity implies the presence of a complex transfer zone between the two master faults, consisting of strike-slip and/or transtensional faults, possibly accomplished by differently oriented secondary normal fault (Barchi et al., 2006). We can invoke the same tectonic setting for the master faults bounding the PM basin (NE dipping) and Agri Valley (SW dipping).

Finally, the delineated system would better explain the high extension rate calculated by historical earthquakes and geodetic data in the study region (Westaway, 1992; Selvaggi, 1998; Anzidei et al., 2001; Hunstad et al., 2003). Considering that this estimate varies between ~2 and ~5 mm/yr for the past centuries, and that the extension rate, measured on individual faults, is significantly lower, a large number of active faults is required rather than a very narrow bands of few faults along the belt with an homogenous geometry.

Acknowledgments

This work has been developed within the 2000-2002 Italian Project "*Probable earthquakes in Italy from year 2000 to 2030: guidelines for determining priorities in seismic risk mitigation*" funded by the National Group for Protection against Earthquakes (*http://gndt.ingv.it/Att_scient/Prodotti_consegnati/prodotti_elenco_progetti_con_int.htm*). Many thanks are due to Riccardo Caputo and an anonymous reviewer for their helpful comments.

References

Amato, A. and Montone, P., 1997. Present-day stress field and active tectonics in southern peninsular Italy. Geophys. J. Int., 130, 519-534.

Anderson, H., and Jackson, J., 1987. Active tectonics of the Adriatic region. Geophys. J. R. Astron. Soc., 91, 937–987.

Anzidei, M., Baldi, P., Casula, G., Galvani, A., Mantovani, E., Pesci, A., Riguzzi, F. & Serpelloni, E., 2001. Insights into present day crustal motion in the central Mediterranean area from GPS surveys. Geophys. J. Int., 146, 98-110.

Barchi, M., Alessandro, A., Cippitelli, G., Merlini, S., and Montone, P., 2006. Extensional tectonics and seismicity in the axial zone of the Southern Apennines. Boll. Soc. Geol. It., Spec. Vol. (in press).

Benedetti, L., Tapponier, P., King, G. C. P. and Piccardi, L., 1998. Surface rupture of the 1857 southern Italian earthquake?. Terra Nova, 10, 206-210.

Casero, P., Roure, F., Endignoux, L., Moretti, I., Muller, C., Sage, L. and Vially, R., 1992. Neogene Geodynamic evolution of the Southern Apennines. Mem. Soc. Geol. Italiana, 41, 109-120.

Castello, B., Selvaggi, G., Chiarabba, C. and Amato, A., 2005. CSI Catalogue of the Italian Seismicity 1981-2002, version 1.0. INGV-CNT, Rome.

Cello, G., Tondi, E., Micarelli, L. and Mattioni, L., 2003. Active tectonics and earthquake sources in the epicentral area of the 1857 Basilicata earthquake (southern Italy). J Geodyn, 36, 37–50.

Cinque, A., Ascione, A. and Chiazzo, C., 2000. Distribuzione spazio-temporale e caratterizzazione della fagliazione quaternaria in Appennino meridionale. In: F. Galadini et al. (eds) Le ricerche del GNDT nel campo della pericolosità sismica (1996-1999), CNR-GNDT, Roma, 2000, 397 pp.

Cinque, A., Patacca, E., Scandone, P. and Tozzi, M., 1993. Quaternary kinematic evolution of the southern Apennines. Relationship between surface geological features and deep lithospheric structures. Ann. Geofis., 36 (2), 249-260.

Cinti, F.R., Faenza, L., Marzocchi, W. and Montone, P., 2004. Probability map of the next M≥ 5.5 earthquakes in Italy. Geochem. Geophys. Geosys., 5, Q11003, doi:10.1029/2004GC000724.

Cinti, F. R., Cucci, L., Pantosti, D., D'Addezio, G. and Meghraoui, M., 1997. A major seismogenic fault in a silent area: The Castrovillari fault (southern Apennines, Italy). Geophys. J. Int., 130, 595–605.

Cocco, M., Chiarabba, C., Di Bona, M., Selvaggi, G., Margheriti, L., Frepoli, A., Lucente, F.P., Basili, A., Jongmans, D. and Campillo, M., 1999. The April 1996 Irpinia seismic sequence: Evidence for fault interaction. J. of Seism., 3, 105–117.

CPTI Working Group, 2004. Catalogo Parametrico dei Terremoti Italiani, versione 2004 (CPTI04). INGV, Bologna. http://emidius.mi.ingv.it/CPTI/

Cucci, L., Pondrelli, S., Frepoli, A., Mariucci, M.T. and Moro, M., 2004. Local pattern of stress field and seismogenic sources in the Pergola-Melandro basin and the Agri Valley (southern Italy). Geophys. J. Int., 156 (3), 575-583.

D'Agostino, N., Giuliani, R., Mattone, M. and Bonci, L., 2001. Active crustal extension in the Central Apennines (Italy) inferred from GPS measurements in the interval 1994-1999. Geophys. Res. Lett., 28 (10), 2121-2124.

De Mets, C., Gordon R.G., Argus, D. F. and Stein, S., 1990. Current plate motions. Geophys. J. Int., 101, 425-478.

DISS Working Group Database of Individual Seismogenic Sources (DISS), Version 3.0.1, 2005. A compilation of potential sources for earthquakes larger than M 5.5 in Italy and surrounding areas. http://www.ingv.it/banchedati/banche.html

Ekström, G., 1994. Teleseismic analysis of the 1990 and 1991 earthquakes near Potenza. Ann. Geofis., 37, 1591-1599.

Frepoli, A., Cinti, F.R., Amicucci, L., Cimini, G.B., De Gori, P. and Pierdominici, S., 2005. Pattern of seismicity and state of stress in the Lucanian Apennines and foredeep (southern Italy) from recording by the Saptex Temporary Array. Ann. Geoph., 48 (6), 1035-1054.

Frepoli, A. and Amato, A., 2000. Fault plane solutions of crustal earthquakes in southern Italy (1988-1995): seismotectonic implications. Ann. Geofis., 43 (3), 437-467.

Galadini, F., Meletti, C. and Vittori, E., 2000. Major active faults in Italy: available surficial data. Netherlands J. of Geosciences, 80 (3/4), 273-296.

Galli, P. and Bosi, V., 2002. Paleoseismology along the Cittanova fault: Implications for seismotectonics and earthquake recurrence in Calabria (southern Italy). J. Geophys. Res., 107(B3), 2044, doi:10.1029/2001JB000234.

Galli, P., Bosi, V., Piscitelli, S., Giocoli, A. and Scionti, V., 2006. Late Holocene earthquakes in southern Apennines: paleoseismology of the Caggiano fault. Int. J. Earth Sci, (Geol. Rundsch) DOI: 10.1007/s00531-005-0066-2.

Giano, S.I. and Martino, C., 2003. Assetto morfotettonico e morfostratigrafico di alcuni depositi continentali pleistocenici del bacino del Pergola-Melandro (Appenino Lucano). Il Quaternario, 16 (2), 289-297.

Hunstad, I., Selvaggi, G., D'Agostino, N., England, P., Clarke, P. and Pierozzi, M., 2003. Geodetic strain in peninsular Italy between 1875 and 2001. Geophys. Res. Let., 30 (4), 1181, doi:10.1029/2002GL016447.

Lippmann-Provansal, M., 1987. L'Apennin meridional (Italie): etude geomorphologique. These de Doct. D'Etat on Geogr. Phys., Univ d'Aix Marseille.

Llera, F. J., Sato, M., Nakatsuka, K. and Yokoyama, H., 1990. Temperature dependence of the electrical resistivity of water-saturated rocks. Geophysics, 55 (5), 576-585.

Loke, M.H. and Barker, R.D., 1996. Rapid least-squares inversion of apparent resistivity pseudosections of a quasi-Newton method. Geophys. Prospec., 44, 131-152

Lucente, F.P., Piana Agostinetti, N., Moro, M., Selvaggi, G. and Di Bona, M., 2005. Possible fault plane in a seismic gap area of southern Apennines (Italy) revealed by receiver function analysis. J. Geophys. Res., 110, B04307, doi: 10.1029/2004JB003187.

Maschio, L., Ferranti, L. and Burrato, P., 2005. Active extension in Val d'Agri area, southern Apennines, Italy: implications for the geometry of the seismogenic belt. Geophysical Journal International, 162 (2), 591-609.

Meletti, C., Patacca, E. and Scandone, P., 2000. Construction of a seismotectonic model: The case of Italy. Pure Appl. Geophys., 157, 11-35.

Menardi Noguera, A. and Rea, G., 2000. Deep structure of the Campanian-Lucanian Arc (southern Appennine, Italy). Tectonophysics, 324 (4), 239-265.

Merlini, S. and Cippitelli, G., 2001. Structural styles inferred by seismic profiles. In: Anatomy of an Orogen: the Apennines and Adjacent Mediterranean Basins (G.B., Vai and I.P., Martini eds), Kluwer Academic Publishers, Great Britain, 441-454.

Michetti, A. M., Ferreli, L., Serva, L. and Vittori, E., 1997. Geological evidence for strong historical earthquakes in an aseismic region: The Pollino case (southern Italy). J. Geodyn., 24, 67-86.

Monaco, C., Tortorici, L. and Paltrineri, W., 1998. Structural evolution of the Lucanian Apennines, southern Italy. J. Struct. Geol., 20 (5), 617-638.

Montone, P., Mariucci, M.T., Pondrelli, S. and Amato, A., 2004. An improved stress map for Italy and surrounding regions (central Mediterranean). J. Geophys. Res., 109, B10410, doi:10.1029/2003JB002703.

Mostardini, F. and Merlini, S., 1986. Appennino centro-meridionale. Sezioni geologiche e proposta di un modello strutturale. Mem. Soc. Geol. Italiana, 35, 177-202.

Pantosti, D., Schwartz, D. P. and Valensise, G., 1993. Paleoseismology along the 1980 Irpinia earthquake fault and implications for earthquake recurrence in the southern Apennines. J. Geophys. Res., 98, 6561-6577.

Patacca, E. and Scandone, P., 2004. The Plio-Pleistocene thrust belt-foredeep system in the southern Apennines and Sicily (southern Apenninic Arc, Italy), in Crescenti U., D'offizi S., Merlini S. and Sacchi R. Eds., Geology of Italy, Spec. Vol. Ital. Geol. Soc. IGC 32 Florence 2004, 93-129.

Pace, B., Peruzza, L., Lavecchia, G. and Boncio, P. 2006. Layered seismogenic source model and probabilistic seismic-hazard analyses in Central Italy. BSSA, 96, 1, 107-132, doi: 10.1785/0120040231.

Pescatore, T., Renda, P., Schiattarella, M. and Tramutoli, M., 1999. Stratigraphic and structural relationships between Meso-Cenozoic Lagonegro basin and coeval carbonate platforms in southern Apennines, Italy. Tectonophysics, 315, 269-286.

Pieri, P., Festa, V., Moretti, M. and Tropeano, M., 1997. Quaternary tectonic activity of the Murge area (Apulian foreland, southern Italy). Annali di Geofisica, 40 (5), 1395-1404.

Pondrelli, S., Morelli, A. and Boschi, E., 1995. Seismic deformation in the Mediterranean area estimated by moment tensor summation. Geophys. J. Int., 122, 938-952.

Pondrelli, S., Morelli, A., Ekström, G., Mazza, S., Boschi, E. and Dziewonski, A.M., 2002. European-Mediterranean regional centroid-moment tensors: 1997-2000. Phys. Earth Planet. Int., 130, 71-101.

Santangelo, N., 1991. Evoluzione geomorfologia e stratigrafica di alcuni bacini lacustri del confine campano-lucano (Italia Meridionale). Tesi di Dott. in Geol. del Sedimentario, III Ciclo, Univ. di Napoli "Federico II", 1-109 pp.

Schiattarella, M., Di Leo, P., Beneduce, P. and Giano, S.I., 2003. Quaternary uplift vs tectonic loading: a case study from the Lucanian Apennine, southern Italy. Quaternary International, 101-102, 239-251.

Selvaggi, G., 1998. Spatial distribution of horizontal seismic strain in the Apennines from historical earthquakes. Ann. Geofis. 41**,** 241-251.

Stuiver, M., Reimer, P.J., Bard, E., Beck, J.W., Burr, G.S., Hughen, K.A., Kromer, B., McCormac, G., van der Plicht, J. and Spurk, M., 1998. INTCAL98 Radiocarbon Age Calibration, 24,000-0 cal BP. Radiocarbon, 40, 1041-1083.

Wells, D. and Coppersmith, K., 1994. New empirical relationships among magnitude, rupture length, rupture width, rupture area and surface displacement. Bull, Seismol. Soc. Am., 84, 974-1002.

Westaway, R., 1992. Seismic moment summation for historical earthquakes in Italy: Tectonic implications. J. Geophys. Res., 97, 15,437-15,464.

Figure Caption

Fig. 1. Historical (yellow square) and instrumental seismicity of the Pergola-Melandro basin and neighbourhood. The 1980 earthquake focal solution, the trace of the seismogenic faults (black lines) in the area and the focal solution of Savoia di Lucania seismic sequence are also shown. At the upper right of the figure is a schematic geological and structural setting of the Lucanian Apennine. Legend: 1- Plio-Quaternary deposits; 2- accrectionary wedge terrains; 3- Meso-Cenozoic neritic carbonates of the Campania-Lucania platform; 4- Lagonegro units; 5- main thrust; 6- main faults.

Fig. 2. Map of the Pergola-Melandro fault (red line). At the lower left are the three profiles performed perpendicular to the fault orientation; they indicate an asymmetry of the basin and mark a sharp change in the angle of the western slope. Profile BB' schematically shows the geological setting of the valley. A significant process of Deep Seated Gravitational Slope Deformation (DSGSD) is ongoing on a sector of the fault and it is responsible for the local convexity of the fault trace. White stars indicate the sites shown in Fig. 3. Legend of the geological profile BB': 1- colluvial and slope deposits (upper Pleistocene-Holocene); 2- Pleistocene alluvial deposits; 3- Lagonegro units; 4- Meso-Cenozoic shallow-water carbonates of the Campania-Lucania platform; 5- main normal faults 6- main thrust.

Fig. 3. a, b – View of the fault scarp in alluvial and colluvial deposits, respectively north and south of the *Brienza* village; **c** - sheared and tilted slope deposits near the village of *S. Angelo Le Fratte*; the sample collected within the deformed deposit is dated 14924-14171 B.C.

Fig. 4. Morpho-structural features identified from photogeological analysis (photo by IGM "Volo Gai 1954", 1:33.000). The photo precedes the quarry. For location of the area see Fig. 2. Legend: 1- drainage pattern; 2- karst-structural depression; 3- landslide; 4- hanging valley; 5- debris fan; 6-

erosional landsurface; 7- flatiron; 8- degraded fault scarp; 9- Pergola-Melandro fault (F1 to F4); 10- inferred fault trace.

Fig. 5. Four branches (F1 to F4) of the southern sector of the Pergola-Melandro fault in a 3D view. The inset at the lower left is an enlargement of the quarry site. We indicate the location of the electrical resistivity profile (dotted line) and of the fault zones exposed at the quarry wall and shown in Figs. 6 and 7.

Fig. 6. View of the upper fault zone (F2) exposed within the quarry in correspondence of the topographic break of the western slope of the Pergola-Melandro basin. The red arrows indicate the sharp tectonic contact between cataclastic dolomia and Upper Quaternary deposits. The age of samples collected within the Quaternary deposits is shown.

Fig. 7. Views of the graben structure at the quarry wall. We overdraw the fault interpretation and the ages of the collected samples. Details of the main fault are shown in (c) and (d).

Fig. 8. 2-D inversion of electrical resistivity data acquired along the profile 1 (see trace in Fig. 5). The acquisition profile is composed by 48 electrodes, 1.5 m spaced both in Dipole-Dipole and Wenner configuration. The apparent resistivity data have been inverted by means of the RES2DINV software (Loke and Barker, 1996), also including the topography with low values of RMS (6% Dipole-Dipole and 2% for Wenner). Both configurations clearly reveal a sharp and steep resistivity discontinuity in correspondence of the surface fault trace F2 and F1.

Table 1 Earthquake parameters in the area of the Pergola-Melandro basin: A) Ma ≥ 5.5 historical events from CPTI Working Group (2004); B) Mw ≥ 4.0 instrumental events from Castello et al, (2005). Imax: Maximum Intensity (MCS scale); Io: epicentral Intensity (MCS scale); Ma: average weight Magnitude; Mw: moment Magnitude. See also the seismicity map in Fig. 1.

A) Ma≥ 5.5 historical events

NAME	Lat	Lon	Year	Month	Day	Time	Min	Imax	Io	Ma
Potenza	40.630	15.800	1273					85	85	5.8
Vallo di Diano	40.520	15.480	1561	8	19	14	10	100	95	6.4
Irpinia-Basilicata	40.880	15.350	1694	9	8	11	40	110	105	6.9
Basilicata	40.520	15.730	1826	2	1	16		90	80	5.6
Basilicata	40.950	15.670	1851	8	14	13	20	100	95	6.3
Irpinia	40.820	15.220	1853	4	9	12	45	90	90	5.9
Basilicata	40.350	15.850	1857	12	16	21	15	110	105	7.0
Irpinia-Basilicata	40.850	15.280	1980	11	23	18	34	100	100	6.9

B) Mw≥ 4.0 instrumental events

NAME	Lat	Lon	Year	Month	Day	Time	Min	Depth (Km)	Mw
Tito	40.618	15.702	1981	1	9	12	50	20.18	4.1
Irpinia	40.861	15.639	1981	1	15	11	12	17.50	4.1
Irpinia	40.838	15.441	1981	1	16	3	7	10.47	4.6
Irpinia	40.754	15.504	1981	3	28	11	1	0.03	4.0
Potenza	40.710	15.728	1981	9	21	16	12	21.99	4.4
Irpinia	40.683	15.497	1982	8	15	15	9	12.00	4.5
Vallo di Diano	40.521	15.593	1983	2	2	8	14	14.84	4.1
Tito	40.642	15.699	1986	7	23	8	19	24.65	4.5
Irpinia	40.823	15.515	1987	1	28	5	33	15.90	4.3
Melandro-Pergola	40.544	15.737	1989	5	29	11	19	0.05	4.0
Potenza	40.640	15.860	1990	5	5	7	21	9-13	5.7
Potenza	40.653	15.850	1990	5	5	7	38	11.34	4.5
Potenza	40.730	15.765	1991	5	26	12	26	11	5.2
Potenza	40.684	15.792	1991	5	26	12		30.28	4.5
Irpinia	40.655	15.442	1996	4	3	13	4	11.43	4.9
Castelluccio-Lauria	40.060	15.949	1998	9	9	11	28	29.21	5.6
Savoia di Lucania	40.585	15.547	2002	4	18	20	56	7.85	4.1

Table 2 Measured and dendrochronologically calibrated 14C age (Stuiver et al., 1998) of collected samples (dating laboratory: Beta Analytic Inc. of Miami, Florida).

SAMPLE	SITE	UNIT	MATERIAL	LAB. CODE	^{14}C Age (yr B.P.)	2σ	Cal. Age BC
B1	F2		Organic silt	Beta-184663	3370+/-40	95.4%	1772-1520
E1	F2		Pedogenic colluvium	Beta-184664	8830+/-50	95.4%	8204-7745
F4CAV-BIS2	F1	A	Paleosoil	Beta-192866	11510+/-60	95.4%	11594-11211
FCAV-CARB2	F1	B	Pedogenic colluvium	Beta-192867	9130+/-40	95.4%	8476-8257
FCAV-2	F1	C	Sandy-silty colluvium	Beta-192864	6640+/-70	95.4%	5639-5480
BR4	S. Angelo Le Fratte		Slope deposits	Beta-192868	13840+/-50	95.4%	14924-14171

Table 3 Parameters of the Pergola-Melandro fault inferred from this work.

LENGTH	STRIKE	DIP	RAKE	MINIMUM LONG TERM SLIP RATE	RECURRENCE TIME
21 km	N320°-N350°	65°-80°	~270°	0.26 mm/yr	~3000 yr

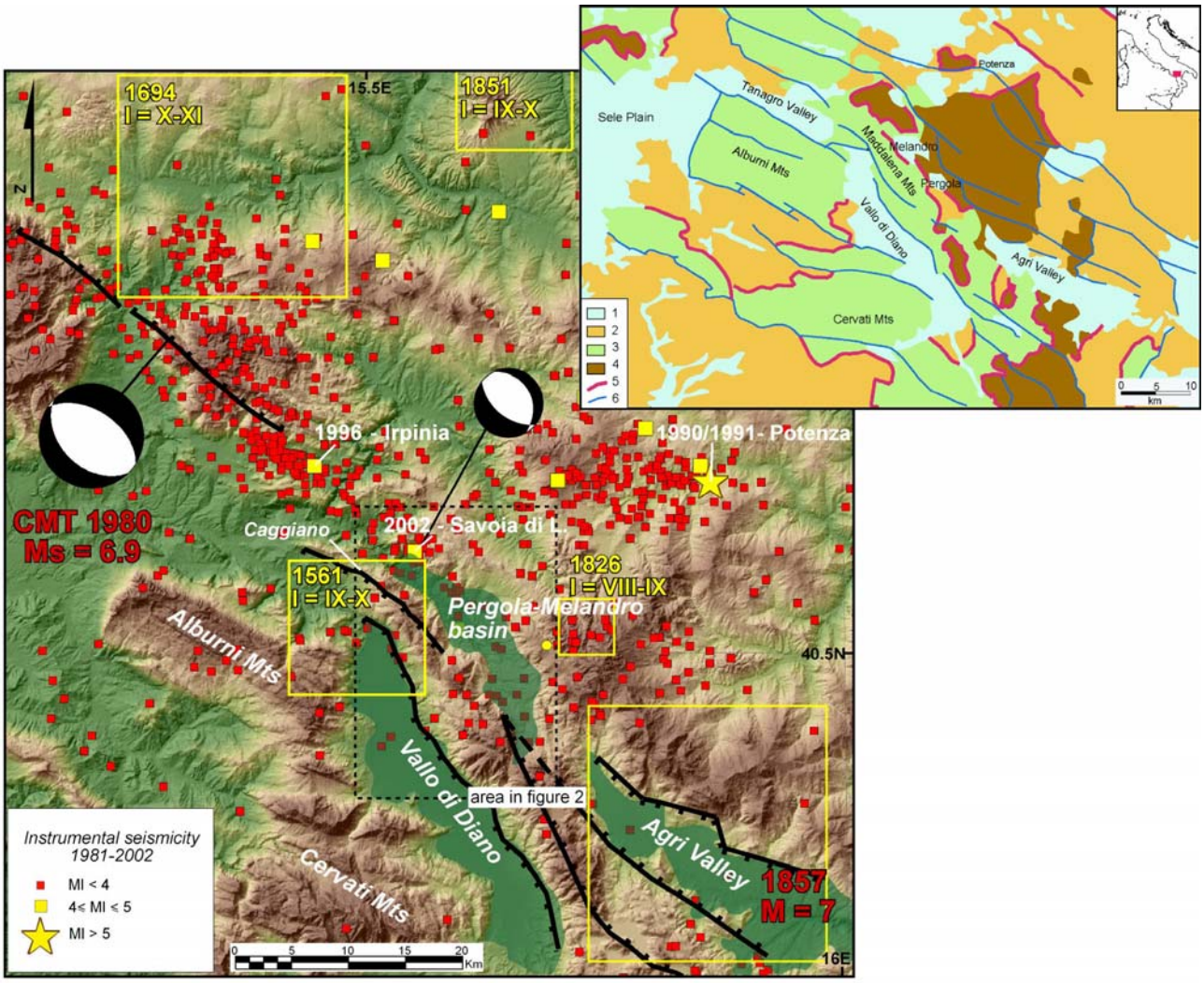
1694
I = X-XI
1851
I = IX-X
15.5E
N
Sele Plain
Tanagro Valley
Alburni Mts
Maddalena Mts
Melandro
Pergola
Vallo di Diano
Agri Valley
Cervati Mts
Potenza
1
2
3
4
5
6
0 5 10
km
1996 - Irpinia
1990/1991- Potenza
CMT 1980
Ms = 6.9
Caggiano
2002 - Savoia di L.
1561
I = IX-X
1826
I = VIII-IX
Pergola-Melandro
basin
Alburni Mts
40.5N
Vallo di Diano
area in figure 2
Agri Valley
1857
M = 7
Cervati Mts
16E
Instrumental seismicity
1981-2002
Ml < 4
4≤ Ml ≤ 5
Ml > 5
0 5 10 15 20
Km

Fig. 1

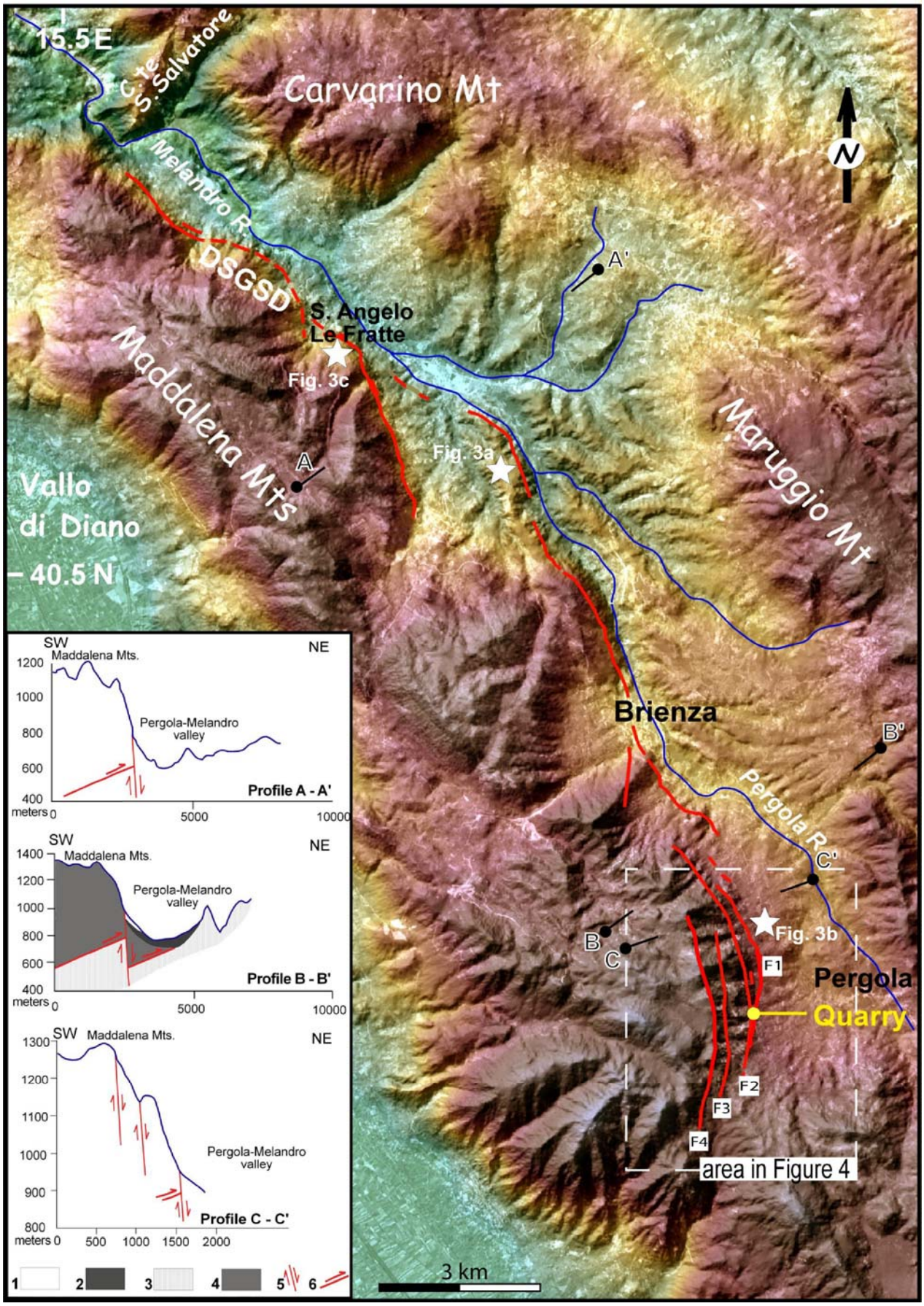
15.5E
C.te S.Salvatore
Carvarino Mt
Melandro R.
DSGSD
S. Angelo Le Fratte
Fig. 3c
Maddalena Mts
A
A'
Fig. 3a
Maruggio Mt
Vallo di Diano
40.5 N
N
Brienza
B'
Pergola R.
C'
Fig. 3b
B
C
F1
Pergola
Quarry
F2
F3
F4
area in Figure 4
3 km
SW
NE
Maddalena Mts.
Pergola-Melandro valley
Profile A - A'
meters
Profile B - B'
Profile C - C'
1
2
3
4
5
6

Fig. 2

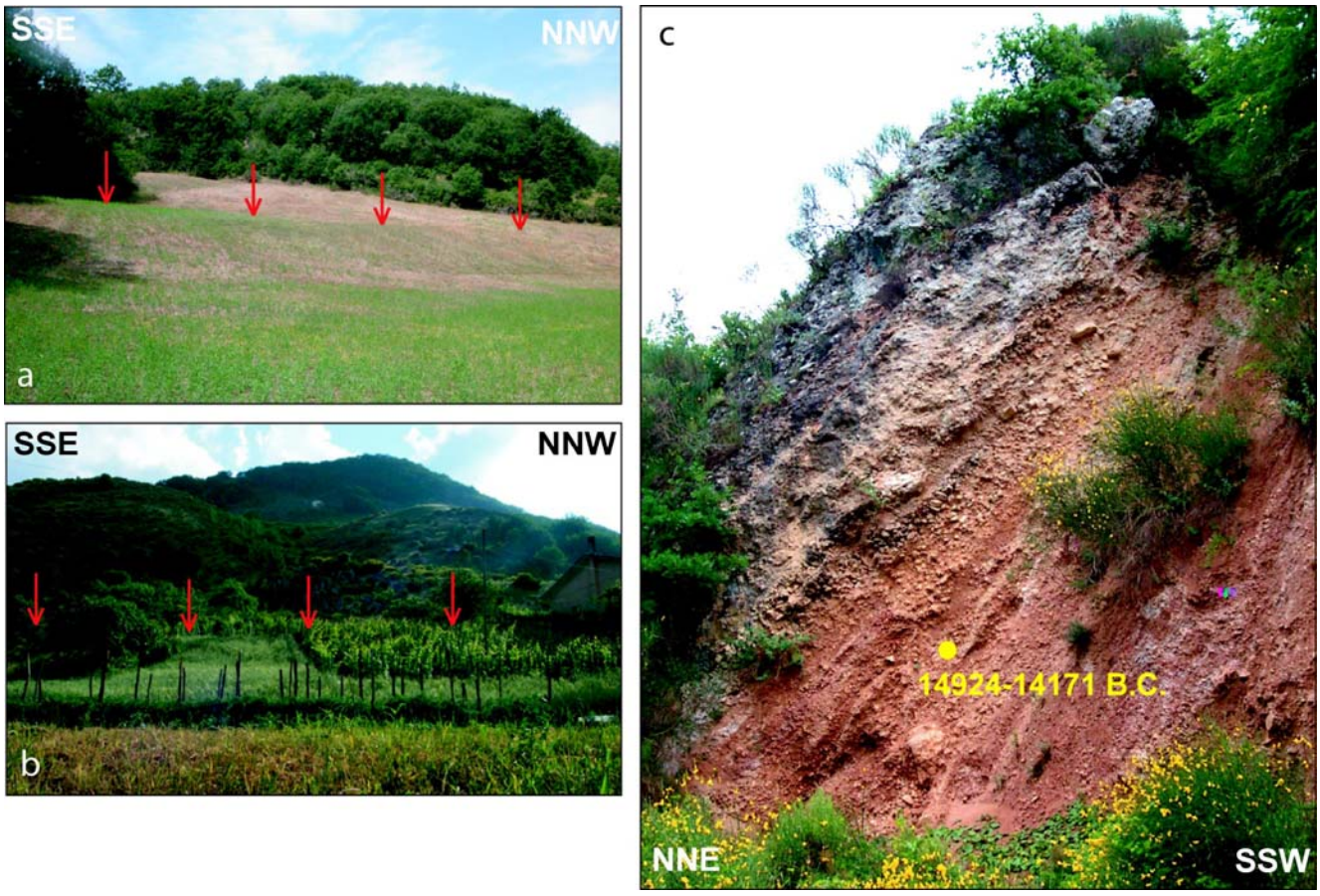

Fig. 3

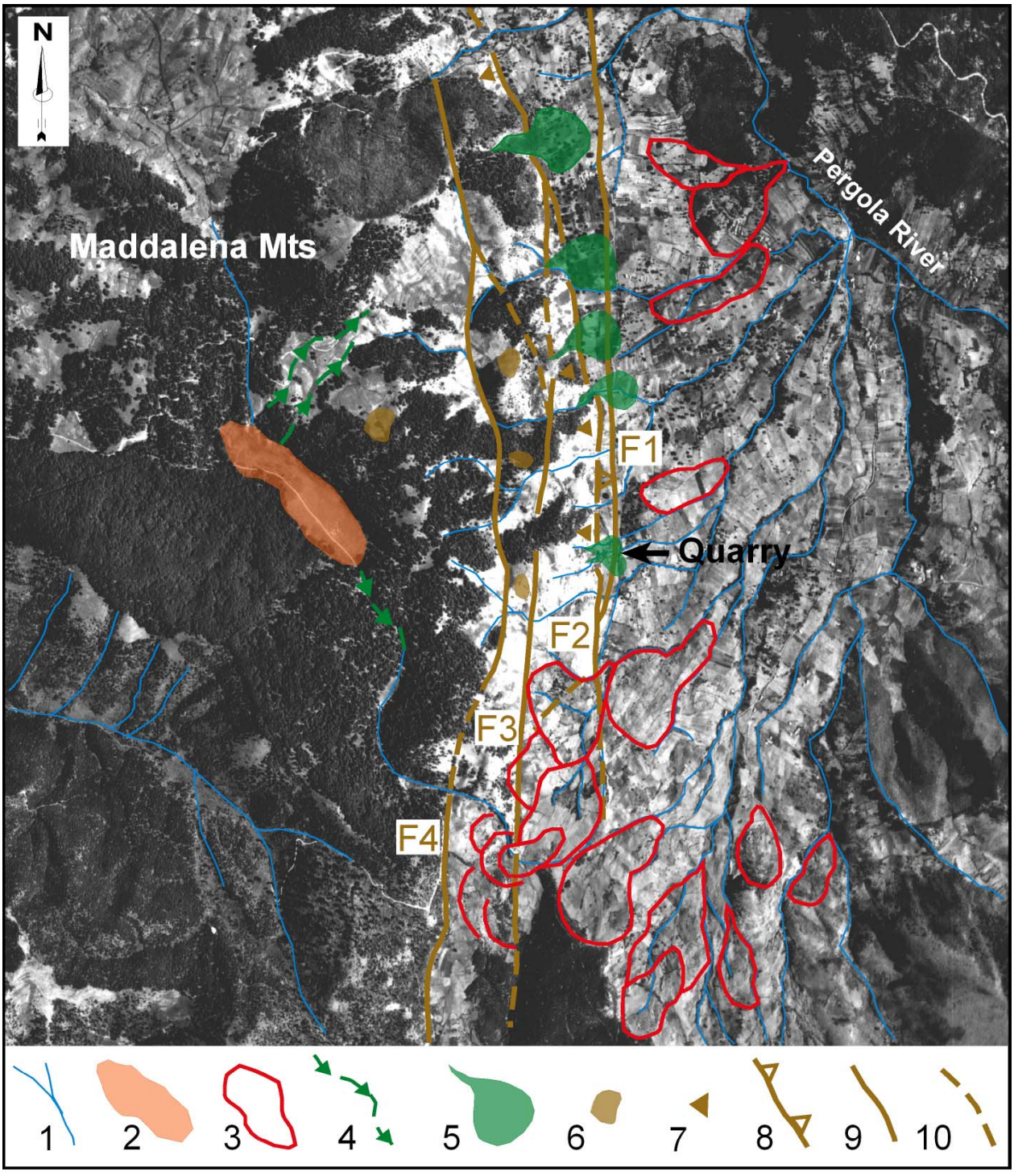
N
Maddalena Mts
Pergola River
F1
Quarry
F2
F3
F4
1
2
3
4
5
6
7
8
9
10

Fig. 4

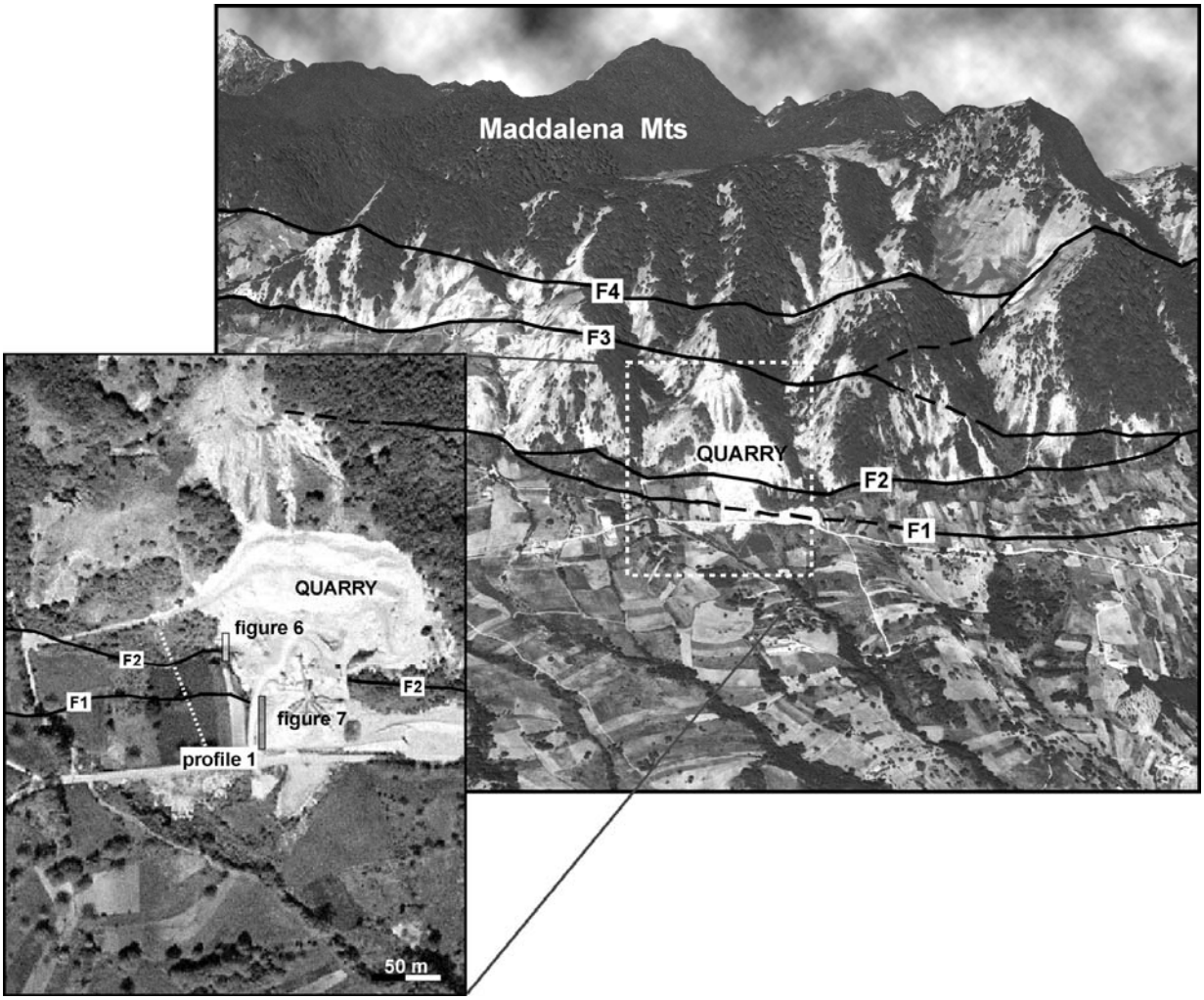
Maddalena Mts
F4
F3
QUARRY
F2
F1
QUARRY
figure 6
F2
F2
F1
figure 7
profile 1
50 m

Fig. 5

Fig. 6

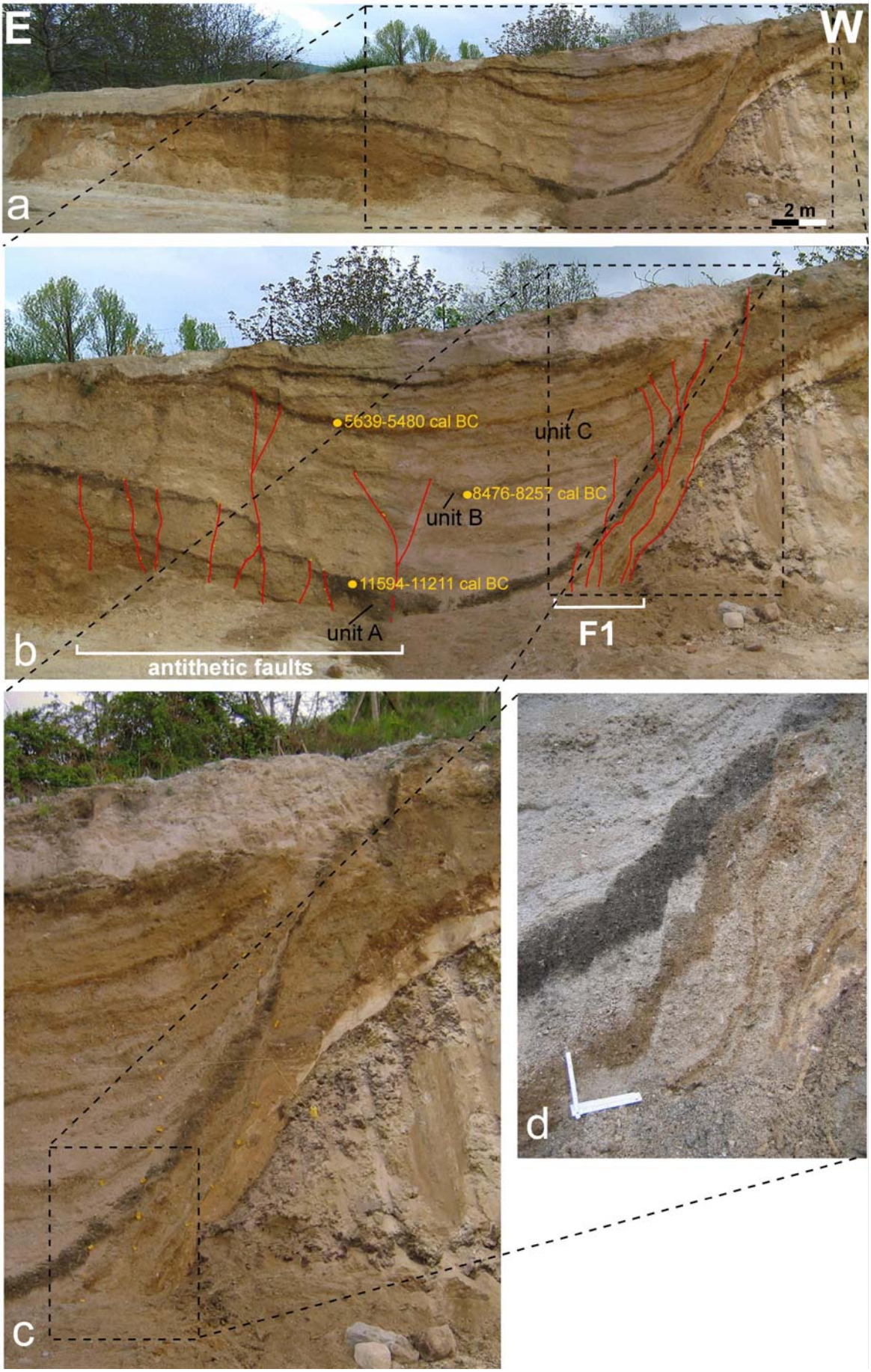
E
W
a
2 m
5639-5480 cal BC
unit C
8476-8257 cal BC
unit B
11594-11211 cal BC
unit A
b
antithetic faults
F1
c
d

Fig. 7

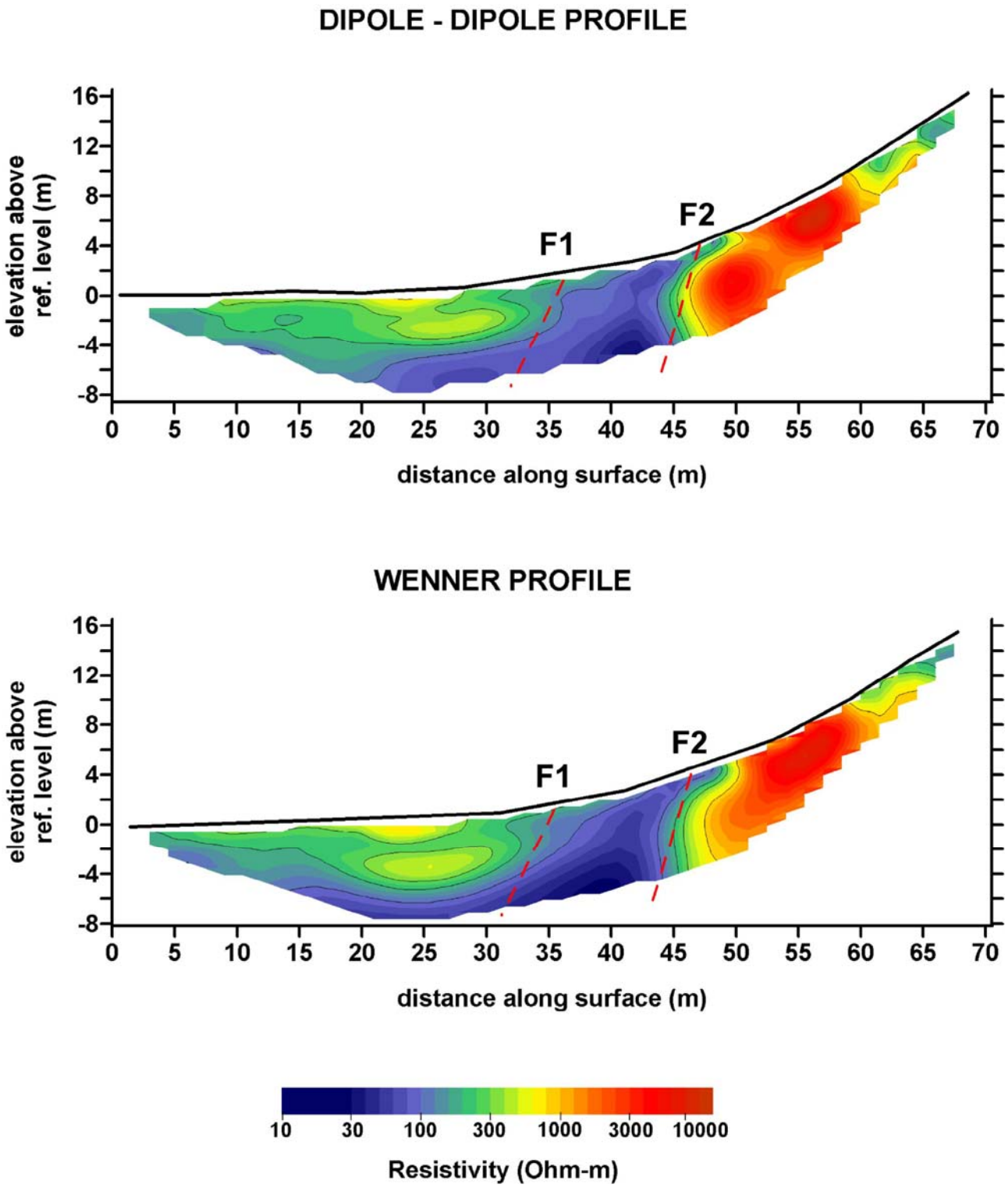
DIPOLE - DIPOLE PROFILE
elevation above ref. level (m)
16
12
8
4
0
-4
-8
F1
F2
0 5 10 15 20 25 30 35 40 45 50 55 60 65 70
distance along surface (m)
WENNER PROFILE
elevation above ref. level (m)
16
12
8
4
0
-4
-8
F1
F2
0 5 10 15 20 25 30 35 40 45 50 55 60 65 70
distance along surface (m)
10 30 100 300 1000 3000 10000
Resistivity (Ohm-m)

Fig. 8